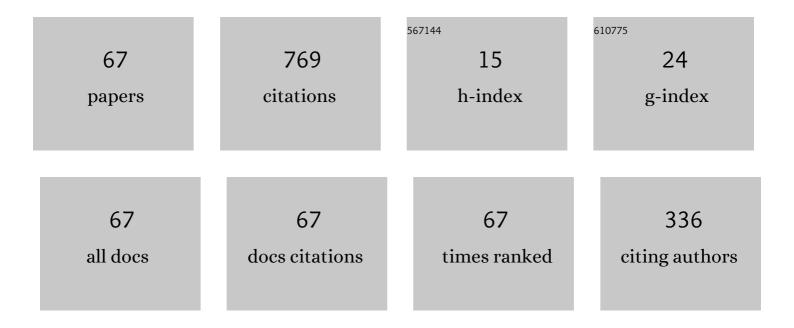
## Zhanchuan Cai

List of Publications by Year in descending order

Source: https://exaly.com/author-pdf/5724131/publications.pdf Version: 2024-02-01



ΖΗΛΝΟΗΠΑΝ ΟΛΙ

#	Article	IF	CITATIONS
1	Re-Evaluating Influence of Rocks on Microwave Thermal Emission of Lunar Regolith Using CE-2 MRM Data. IEEE Transactions on Geoscience and Remote Sensing, 2022, 60, 1-12.	2.7	9
2	High-Resolution Feature Pyramid Network for Automatic Crater Detection on Mars. IEEE Transactions on Geoscience and Remote Sensing, 2022, 60, 1-12.	2.7	12
3	Modeling of Crater Group Representation Based on V-System. IEEE Transactions on Geoscience and Remote Sensing, 2022, 60, 1-12.	2.7	0
4	TEBCF: Real-World Underwater Image Texture Enhancement Model Based on Blurriness and Color Fusion. IEEE Transactions on Geoscience and Remote Sensing, 2022, 60, 1-15.	2.7	18
5	ICHV: A New Compression Approach for Industrial Images. IEEE Transactions on Industrial Informatics, 2022, 18, 4427-4435.	7.2	4
6	MFFN: An Underwater Sensing Scene Image Enhancement Method Based on Multiscale Feature Fusion Network. IEEE Transactions on Geoscience and Remote Sensing, 2022, 60, 1-12.	2.7	21
7	An Information Security Method Based on Optimized High-Fidelity Reversible Data Hiding. IEEE Transactions on Industrial Informatics, 2022, 18, 8529-8539.	7.2	4
8	A Novel Spline Algorithm Applied to COVID-19 Computed Tomography Image Reconstruction. IEEE Transactions on Industrial Informatics, 2022, 18, 7804-7813.	7.2	3
9	Potential Applications of CE-2 Microwave Radiometer Data in Understanding Basaltic Volcanism in Heavily Ejecta-Contaminated Mare Frigoris. Remote Sensing, 2022, 14, 2725.	1.8	4
10	High-Fidelity Reversible Image Watermarking Based on Effective Prediction Error-Pairs Modification. IEEE Transactions on Multimedia, 2021, 23, 52-63.	5.2	21
11	A Novel Image Representation Method Under a Non-Standard Positional Numeral System. IEEE Transactions on Multimedia, 2021, 23, 1301-1315.	5.2	2
12	High Capacity Reversible Data Hiding in Encrypted Image Based on Intra-Block Lossless Compression. IEEE Transactions on Multimedia, 2021, 23, 1466-1473.	5.2	36
13	Absolute model age of lunar Finsen crater and geologic implications. Icarus, 2021, 354, 114046.	1.1	15
14	YuvConv: Multi-Scale Non-Uniform Convolution Structure Based on YUV Color Model. IEEE Transactions on Multimedia, 2021, 23, 2533-2544.	5.2	0
15	Efficient Reconstruction of Industrial Images Using Optimized HMK Splines. IEEE Transactions on Industrial Informatics, 2021, 17, 4657-4668.	7.2	2
16	A Single Neural Network for Mixed Style License Plate Detection and Recognition. IEEE Access, 2021, 9, 21777-21785.	2.6	26
17	Reunderstanding Geomorphological Features in Chang'e-5 Sampling Region Based on Multiscale Roughness Model. IEEE Journal of Selected Topics in Applied Earth Observations and Remote Sensing, 2021, 14, 9106-9116.	2.3	1
18	Reversible Data Hiding Based on Dual Pairwise Prediction-Error Expansion. IEEE Transactions on Image Processing, 2021, 30, 5045-5055.	6.0	46

ZHANCHUAN CAI

#	Article	IF	CITATIONS
19	A New Image Compression Algorithm Based on Non-Uniform Partition and U-System. IEEE Transactions on Multimedia, 2021, 23, 1069-1082.	5.2	15
20	Special Thermophysical Features of Floor Materials in Mare Smythii Indicated by CE-2 CELMS Data. IEEE Journal of Selected Topics in Applied Earth Observations and Remote Sensing, 2021, 14, 8135-8143.	2.3	6
21	Modeling of Lunar Digital Terrain Entropy and Terrain Entropy Distribution Model. IEEE Transactions on Geoscience and Remote Sensing, 2021, 59, 1052-1066.	2.7	2
22	Mare basalt flooding events surrounding Chang'e-4 landing site as revealed by Zhinyu crater ejecta. Icarus, 2021, 360, 114370.	1.1	9
23	Evaluation of the day-time ground-level turbulence at Mt Wumingshan with a microthermal sensor. Monthly Notices of the Royal Astronomical Society, 2021, 505, 3070-3077.	1.6	9
24	Linear Independence of T-Spline Blending Functions of Degree One for Isogeometric Analysis. Mathematics, 2021, 9, 1346.	1.1	1
25	Planar Typical Bézier Curves with a Single Curvature Extremum. Mathematics, 2021, 9, 2148.	1.1	2
26	An Underwater Image Vision Enhancement Algorithm Based on Contour Bougie Morphology. IEEE Transactions on Geoscience and Remote Sensing, 2021, 59, 8117-8128.	2.7	43
27	Severity Assessment of COVID-19 Based on Feature Extraction and V-Descriptors. IEEE Transactions on Industrial Informatics, 2021, 17, 7456-7467.	7.2	15
28	An Image Importance Partition-based Compression Method for COVID-19 Computed Tomography Scan. IEEE Transactions on Industrial Informatics, 2021, , 1-1.	7.2	0
29	A Generalized Walsh System and Its Fast Algorithm. IEEE Transactions on Signal Processing, 2021, 69, 5222-5233.	3.2	3
30	A New Approach for Character Recognition of Multi-Style Vehicle License Plates. IEEE Transactions on Multimedia, 2021, 23, 3768-3777.	5.2	18
31	Evaluating a Special Lunar TIR Cold Anomaly Using CE-2 CELMS Data. , 2021, , .		0
32	New Insights into a Rock-Related TIR Anomaly on the Moon from CE-2 Celms Satellite Data. , 2021, , .		0
33	Typical curve with G1 constraints for curve completion. Visual Computing for Industry, Biomedicine, and Art, 2021, 4, 28.	2.2	0
34	Designing planar cubic B-spline curves with monotonic curvature for curve interpolation. Computational Visual Media, 2020, 6, 349-354.	10.8	3
35	Daytime optical turbulence profiling with a profiler of the differential solar limb. Monthly Notices of the Royal Astronomical Society, 2020, 499, 1909-1917.	1.6	14
36	Complex Mare Deposits Revealed by CE-2 CELMS Data in Mare Nubium. IEEE Journal of Selected Topics in Applied Earth Observations and Remote Sensing, 2020, 13, 2475-2484.	2.3	6

ZHANCHUAN CAI

#	Article	IF	CITATIONS
37	An Insight into Pixel Value Ordering Prediction Based Prediction-error Expansion. IEEE Transactions on Information Forensics and Security, 2020, , 1-1.	4.5	11
38	Mare Deposits Identification and Feature Analysis in Mare Australe Based on CEâ€2 CELMS Data. Journal of Geophysical Research E: Planets, 2020, 125, e2019JE006330.	1.5	7
39	Reevaluating Mare Moscoviense And Its Vicinity Using Chang'e-2 Microwave Sounder Data. Remote Sensing, 2020, 12, 535.	1.8	20
40	Flexible spatial location-based PVO predictor for high-fidelity reversible data hiding. Information Sciences, 2020, 520, 431-444.	4.0	24
41	A New Class of Explicit Interpolatory Splines and Related Measurement Estimation. IEEE Transactions on Signal Processing, 2020, 68, 2799-2813.	3.2	6
42	Re-Evaluating Basaltic Deposits in Mare Nubium with CE-2 CELMS Data. , 2020, , .		0
43	A Novel Shape Representation Method for Complex Trademark Image. IEEE Access, 2019, 7, 53800-53811.	2.6	5
44	Cardinal MK-spline signal processing: Spatial interpolation and frequency domain filtering. Information Sciences, 2019, 495, 116-135.	4.0	12
45	A Novel Stitching Method for Dust and Rock Analysis Based on Yutu Rover Panoramic Imagery. IEEE Journal of Selected Topics in Applied Earth Observations and Remote Sensing, 2019, 12, 4457-4466.	2.3	5
46	An Improved Skeleton Extraction Method via Multi-Task and Variable Coefficient Loss Function in Natural Images. IEEE Access, 2019, 7, 171272-171284.	2.6	3
47	A New High Capacity Separable Reversible Data Hiding in Encrypted Images Based on Block Selection and Block-Level Encryption. IEEE Access, 2019, 7, 175671-175680.	2.6	11
48	An Adaptive Triangular Partition Algorithm for Digital Images. IEEE Transactions on Multimedia, 2019, 21, 1372-1383.	5.2	7
49	Measuring Multiresolution Surface Roughness Using V-System. IEEE Transactions on Geoscience and Remote Sensing, 2018, 56, 1497-1506.	2.7	5
50	Potential Geologic Significances of Hertzsprung Basin Revealed by CE-2 CELMS Data. IEEE Journal of Selected Topics in Applied Earth Observations and Remote Sensing, 2018, 11, 3713-3720.	2.3	13
51	Improved Multiscale Roughness Algorithm for Lunar Surface. IEEE Journal of Selected Topics in Applied Earth Observations and Remote Sensing, 2018, 11, 2336-2345.	2.3	4
52	Passive Microwave Probing Mare Basalts in Mare Imbrium Using CE-2 CELMS Data. IEEE Journal of Selected Topics in Applied Earth Observations and Remote Sensing, 2018, 11, 3097-3104.	2.3	33
53	Lunar Brightness Temperature Map and TB Distribution Model. IEEE Transactions on Geoscience and Remote Sensing, 2018, 56, 7310-7323.	2.7	12
54	Reversible data hiding using multi-pass pixel-value-ordering and pairwise prediction-error expansion. Information Sciences, 2018, 467, 784-799.	4.0	57

ZHANCHUAN CAI

#	Article	IF	CITATIONS
55	Microwave Thermal Emission at Tycho Area and Its Geological Significance. IEEE Journal of Selected Topics in Applied Earth Observations and Remote Sensing, 2017, 10, 2984-2990.	2.3	27

## Automatic stitching method for Chang'E-2 CCD images of the Moon. Journal of Earth Science (Wuhan,) Tj ETQqQ 0 0 rgB¼ /Overlock

57	Hierarchical MK Splines: Algorithm and Applications to Data Fitting. IEEE Transactions on Multimedia, 2017, 19, 921-934.	5.2	8
58	Correlation Analysis Between Lunar Surface Roughness and Other Land-Surface Parameters Using BPNN. IEEE Journal of Selected Topics in Applied Earth Observations and Remote Sensing, 2017, 10, 5647-5656.	2.3	3
59	Lunar Brightness Temperature Model Based on the Microwave Radiometer Data of Chang'e-2. IEEE Transactions on Geoscience and Remote Sensing, 2017, 55, 5944-5955.	2.7	36
60	Microwave thermal emission features of Mare Orientale revealed by CELMS data. , 2016, , .		2
61	Influence of (FeO+TiO2) abundance on the microwave thermal emissions of lunar regolith. Science China Earth Sciences, 2016, 59, 1498-1507.	2.3	34
62	Research on microwave thermal emission at Tycho area and its geological significance. , 2016, , .		0
63	Orthogonal Polar V Transforms and application to shape retrieval. Journal of Visual Communication and Image Representation, 2016, 34, 146-152.	1.7	1
64	Lunar surface roughness based on multiscale morphological method. Planetary and Space Science, 2015, 108, 13-23.	0.9	16
65	Fractal structure of lunar topography: An interpretation of topographic characteristics. Geomorphology, 2015, 238, 112-118.	1.1	14
66	Automatic seamless stitching method for CCD images of Chang'E-1 lunar mission. Journal of Earth Science (Wuhan, China), 2011, 22, 610-618.	1.1	8
67	Lunar digital elevation model and elevation distribution model based on Chang'E-1 LAM data. Science China Technological Sciences, 2010, 53, 2558-2568.	2.0	11